

# Crystallization of Single Molecule Magnets by Compressed Fluids with Control of Particle Size and Morphology

M. Munto,<sup>a</sup> J. Gomez,<sup>a</sup> J. Campo,<sup>b</sup> D. Ruiz-Molina,<sup>a</sup> N. Ventosa,\*<sup>a</sup> J. Veciana<sup>a\*</sup>

<sup>a</sup> Departament de Nanociència Molecular i Materials Orgànics. Institut de Ciència de Materials de Barcelona (ICMAB- CSIC).

Campus de la Universitat Autònoma de Barcelona, Bellaterra E-08193 (Catalonia, Spain)

<sup>b</sup> Departamento de Física de la Materia Condensada. Instituto de Ciencia de Materiales de Aragón (ICMA-CSIC-Universidad de Zaragoza)

c/ Pedro Cerbuna 12, Zaragoza 50009 (Aragón, Spain)

Corresponding Author [vecianaj@icmab.es](mailto:vecianaj@icmab.es), [ventosa@icmab.es](mailto:ventosa@icmab.es)

Fax (+34) 93 580 57 29

**Abstract** Microparticles of the Single Molecule Magnet (SMM)  $[\text{Mn}_{12}\text{O}_{12}(\text{O}_2\text{C}_6\text{H}_5)_{16}(\text{H}_2\text{O})_4]$  ( $\text{Mn}_{12}$ ) with controlled size and polymorphism have been prepared by GAS crystallization technique, showing a remarkable particle size influence on the magnetization relaxation rates.

## INTRODUCTION

Single Molecule Magnets (SMMs) have attracted considerable attention in recent times, where each molecule displays magnetic properties normally associated with mesoscale magnetic particles.<sup>1</sup> The origin for such behavior lies in the combination of a large-spin ground state with appreciable magnetic anisotropy, resulting in a barrier for the spin reversal.<sup>1</sup> As a consequence, interesting magnetic properties such as out-of-phase ac magnetic susceptibility signals, magnetization hysteresis loops<sup>2</sup> and resonant magnetization tunneling, have been reported.<sup>3</sup>

Although the origin of SMMs magnetic properties has been unequivocally attributed to individual molecules rather than to the existence of long range magnetic intermolecular interactions, they have been shown to be very dependent on structural and crystalline restrictions. For instance, previous works have shown the influence of dislocations on the resonant spin tunneling of a crystal of  $\text{Mn}_{12}$  clusters<sup>4</sup> or the existence of at least two different magnetization relaxation processes,<sup>5</sup> being them highly influenced by the crystalline network characteristics.<sup>6</sup> For these reasons, the preparation of crystalline samples of SMMs with controlled structural parameters, such as morphology, size and polymorphism, has become a challenge. If successful, this will give us a unique opportunity to study the influence of such structural parameters on the magnetic properties of SMMs crystals.

So far, these metal-organic clusters are crystallized using conventional crystallization techniques, for instance, the slow diffusion of an anti-solvent over cluster solutions. These methods exhibit only a limited control of particle size distribution and polymorphic purity, often obtaining mixtures of large crystals with wide particle size distributions, different morphologies and/or mixtures of different crystal structures that occlude solvent molecules in the crystal network. Moreover, guest solvent elimination promotes crystal rupturing and fragmentation, enlarging even more the particle size distribution of the original material. Consequently, these techniques are not suitable for obtaining powders with controlled particle size and polymorphic nature.

One of the most effective crystallization methodologies used over the last decade is based on the use of supercritical fluids.<sup>7</sup> Compressed fluid, have allowed the straightforward

preparation of crystalline solids with microscopic and nanoscopic monodisperse particle size and polymorphic purity. In these crystallization procedures, large supersaturation levels are attained over short periods of time, favoring the preparation of crystalline solids with small particle size and narrow particle distributions. Moreover, since crystallization takes place far from stable thermodynamic situations, the obtaining of kinetically favored polymorphic forms is enhanced. However, as far as we know, it has never been used before for the controlled crystallization of SMMs.

In this work we report the controlled crystallization of complex  $[\text{Mn}_{12}\text{O}_{12}(\text{O}_2\text{C}_6\text{H}_5)_{16}(\text{H}_2\text{O})_4]$  (**1**) by the Gas Anti-Solvent crystallization technique (GAS), that utilizes compressed  $\text{CO}_2$  as an anti-solvent,<sup>8</sup> in order to obtain crystalline samples with high polymorphic purity, controlled particle size and narrow size distribution, which will be used to study the influence of the particle size on the magnetization relaxation rates and its relevance on future experimental magnetization studies.<sup>9</sup>

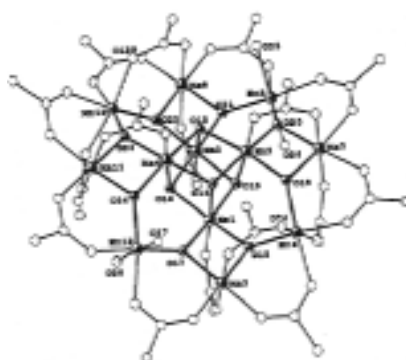


**Figure 1.** Representation of the core of complex  $[\text{Mn}_{12}\text{O}_{12}(\text{O}_2\text{C}_6\text{H}_5)_{16}(\text{H}_2\text{O})_4]$  (**1**). The terminal benzene rings are not showed.

## MATERIALS AND METHODS

Complex **1** was prepared as previously described in the literature and purified by recrystallization from diffusion of n-hexane over chloroform. Chloroform of Gradient Quality was purchased from Teknokroma (Barcelona, Spain). N-hexane of Syntheses Quality was purchased from SDS (Peypin, France). Carbon Dioxide was supplied by Carbueros Metálicos S.A – Air Products (Barcelona, Spain).

A scheme of the experimental apparatus used to perform all experiments is illustrated in Figure 2. The liquefied carbon dioxide was pumped using a diaphragm pump (DOSAPRO MILTON ROY, Point Saint-Pierre, France) after being cooled with a heat exchanger, S1, to prevent cavitations. The amount of carbon dioxide introduced in the vessel was measured using a mass flowmeter (Optimassmfm 7150K/01S, KRONE, Germany), Q. After pumped, the  $\text{CO}_2$  was heated to the desired temperature in a spiral heat exchanger, S2, before being introduced into the high-pressure vessel. The autoclave temperature was measured using a stainless steel thermocouple placed inside the vessel. Temperature was kept constant through a controlled temperature water-glycol jacket. The pressure was measured by means of a pressure transducer placed in the vessel. The autoclave, R1 (Autoclave Engineers, Erie, USA) consisting on a stainless steel jacketed vessel of 300 ml, was equipped with a stirrer driven by an electromagnetic motor (Autoclave Engineers, Erie, USA). A stainless steel filter

housing (Headline Filters, UK), F1, was placed at the exit of the crystallizer to collect crystals after precipitation.

Valves, temperature controllers and manometers complete the system.

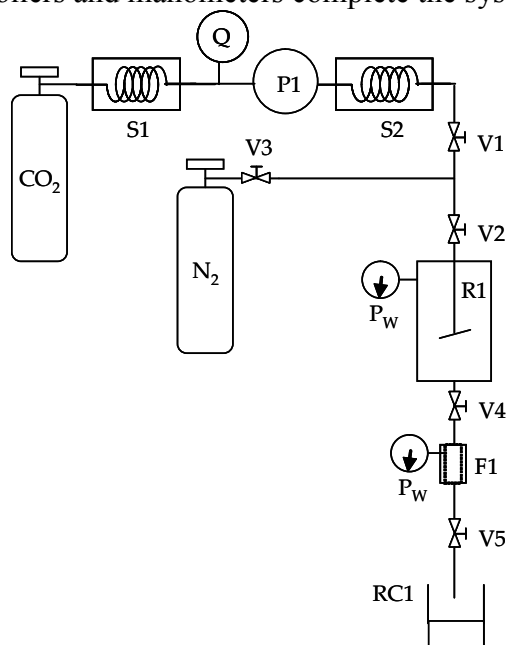


**Figure 2.** Scheme of the equipment used in GAS crystallization experiments. P: pump; S: heat exchanger; Q: flowmeter, V: valve; F: filter; R: crystallizer; RC: recycling collector.

A dissolution of the complex at the working temperature  $T_w$  with a given supersaturation ratio,  $\beta$ , was introduced into the vessel. The dissolution was pressurized at  $P_w$ , adding  $CO_2$  at a given flow,  $Q_{CO_2}$ . The working temperature,  $T_w$ , was kept constant through a controlled temperature water-glycol jacket. The mixture was stirred at a given speed,  $\omega$ , in order to ensure a complete homogenization. By gradual pressurization, the gas was dissolved in the liquid dissolution until the system reached the final expansion. As the  $CO_2$  was dissolved, the equilibrium solubility was lowered and the solid precipitated. After precipitation, the crystals were collected in a concentric filter placed at the exit of the vessel. In order to keep constant the pressure of the system during the filtration process, fresh  $N_2$  was introduced from the top of the vessel during the filtration step. Finally, the system was gradually depressurized. The precipitation yield was determined by gravimetric analysis. The purity of the GAS precipitates was determined by Elemental Analysis, its solvent content was measured by Termogravimetric Analysis (TG), the particle morphology was observed by Scanning Electron Microscopy (SEM), its crystallinity was analyzed by X-Ray Powder Diffraction (XRPD) and the sample particle size distribution was determined by Laser Scattering (LS).

## RESULTS AND DISUSSION

Several GAS crystallization experiments of complex **1** from chloroform/ $CO_2$  solvent mixtures were carried out using the equipment and experimental procedure described in the previous

section. The operational parameters used in each experiment, as well as the crystallization yield and the particle characteristics of the solids obtained, are summarized in Table 1. From here, it can be inferred that all GAS processed samples have a particle uniformity index one order of magnitude higher than that corresponding to the sample obtained by conventional diffusion crystallization technique, in which chloroform was used as solvent and hexane as antisolvent.

**Table 1.** GAS crystallizations experiments of the complex  $Mn_{12}$  from chloroform/ $CO_2$  solvent mixtures at an initial supersaturation ratio  $\beta=0.9$ ,  $P_W = 10$  MPa and  $T_W = 298$  K.

Exp	$X_W$	$\omega$ (rpm)	GAS yield (%)	Diameter of particles ( $\mu m$ ) <sup>a</sup>			U.I <sup>c</sup>
				D(0.1)	D(0.5) <sup>b</sup>	D(0.9)	
GAS 1	0.4	1000	5	-	-	-	-
GAS 2	0.53	1000	30	5	30	65	8
GAS 3	0.69	500	50	5	25	50	10
GAS 4	0.69	1000	55	5	20	40	13
GAS 5	0.69	1500	60	5	20	40	13
GAS 6	0.82	1000	75	5	15	35	15
Raw $Mn_{12}$ <sup>d</sup>	-	-	-	2	50	125	1

The flow rate of  $CO_2$ , during the pressurization step, used in all experiments was 0.8 Kg/h.

<sup>a</sup> Volumetric particle size distributions, measured with Laser Scattering technique (Beckman-Coulter LS 13320, USA), are given as 10, 50 and 90% quantiles.

<sup>b</sup> These values correspond to the medians of the particle distributions. The average diameters of particles were confirmed by SEM images (vide infra).

<sup>c</sup> The Uniformity Index (IU) is defined as  $D(0.1)/D(0.9) * 100$ . The higher is the IU, the narrower is the particle size distribution.

<sup>d</sup> Sample of complex  $Mn_{12}$  obtained by a standard diffusion of *n*-hexane into  $CHCl_3$ . The particle size measurements were carried out using already fragmentized crystals. Fragmentation phenomena start as the sample was removed from the mother liquor.

From the results of experiments GAS1, GAS2, GAS4 and GAS6, where all operational parameters were kept constant except  $X_W$ , we have observed that the higher is the amount of  $CO_2$  introduced, the narrower is the particle size distribution. Moreover, as can be ascertained by the SEM images shown in Figure 3, GAS solids have uniform morphologies, although strongly dependent on the  $CO_2$  content. For instance, cubic morphologies are obtained at medium  $CO_2$  molar fractions (GAS 2) and plates at higher molar fractions (GAS 4). As expected, we have observed that the higher is the  $CO_2$  concentration,  $X_W$ , the smaller are the particles produced. Indeed as higher is the  $CO_2$  content higher is the maximum supersaturation attained, and the nucleation process is more enhanced over crystal growth, with the obtaining of smaller particles.

Experiments GAS 3 and GAS 5 only differ in the stirring rate used. As it can be inferred from results of Table 1, by changing this operational parameter, it was observed a only a slightly decrease on particle sizes when going from 500 to 1000 rpm. This suggests that the kinetic of  $CO_2$  dissolution into chloroform is the limiting factor for determining the minimum achievable particle size.

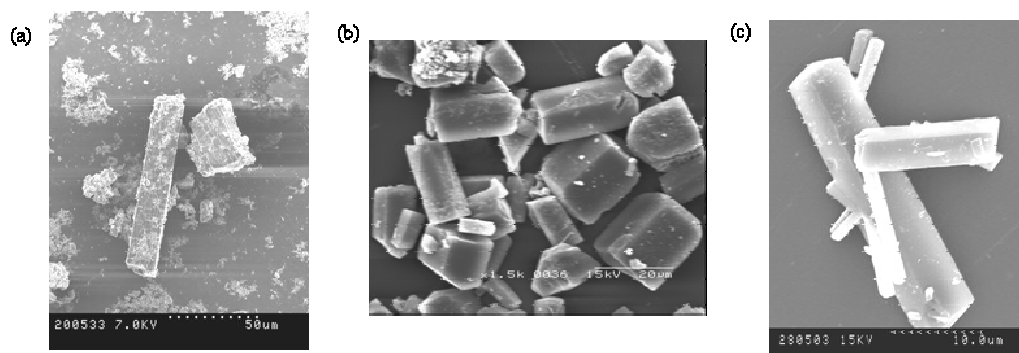


**Figure 3.** SEM images of  $Mn_{12}$  solids obtained by: slow diffusion of n-hexanes over a complex dissolution in chloroform with an initial supersaturation ratio  $\beta=0.9$  (a), GAS precipitation in experiments GAS2 (b) and GAS 4(c).

As ascertained by powder X-Ray diffraction, the resulting GAS microparticles are crystalline (see **Figure 4**), although their diffraction patterns exhibit considerable differences with that observed for the sample obtained by diffusion of hexane into chloroform. After a careful bibliographic search, we can conclude that the crystallographic phase obtained in all the GAS samples was not described previously. Moreover, elemental and thermal analysis confirms the lack of crystallization solvent molecules within the crystal network.

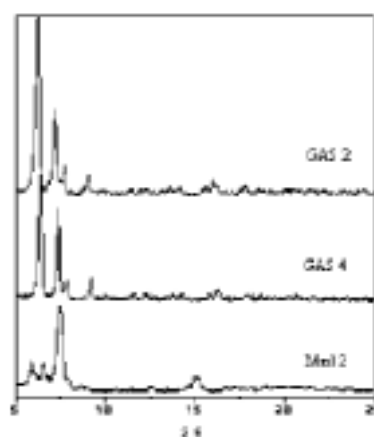


**Figure 4.** X-Ray Powder diffractograms of conventionally crystallized  $Mn_{12}$  (bottom), solid obtained in GAS 4 (middle) and GAS 2 (top).

## CONCLUSIONS

Using the GAS technique we were able to produce stable solid samples of complex **1** with a controlled particle size, more than one order of magnitude smaller than that achieved by conventional diffusion crystallization, and with a narrower particle size distribution. In addition the particles produced, have no solvent voids, and they have a crystalline structure never described before. These results encourage the use of precipitation with compressed fluids for the obtaining of stable crystalline samples of SMMs with different particle sizes and polymorphism, to study the influence of these structural parameters on the magnetic properties of these materials.

## AKNOWLEDGEMENTS

This work was supported by DGI (Spain) under projects MAT2002-0043 and by the European Commission under the NoE MAGMANET (Contract NMP3-CT-2005-515767) and QUEMOLNA Marie Curie RTN (Contract MRTN-CT-2003-5044880). Dr.Javier Campo and Dr.Nora Ventosa thank de Ministerio de Educaión y Ciencia (Spain) for their Ramon y Cajal contracts.

## REFERENCES

- [1] (a) G. Christou, D. Gatteschi, D. N. Hendrickson, and R. Sessoli, *MRS Bull.* 25, **2000**, 56. (b) D. Gatteschi and R. Sessoli, *Angew. Chem. Int. Ed.*, 42, **2003**, 268.
- [2] (a) R. Sessoli, D. Gatteschi, A. Caneschi, A. Novak, *Nature*, 365, **1993**, 141. (b) D. Gatteschi, A. Caneschi, L. Pardi, R. Sessoli, *Science*, 265, **1994**, 1054.
- [3] (a) J. R. Friedman, M. P. Sarachik, J. Tejada, and R. Ziolo, *Phys. Rev. Lett.*, 76, 1996, 3830. (b) J.M. Hernández, X.X. Zhang, F. Luis, J. Bartolomé, J. Tejada, R. Ziolo, *Europhys. Lett.*, 35, **1996**, 301. (c) L. Thomas, F. Lioni, R. Ballou, D. Gatteschi, R. Sessoli, B. Barbara, *Nature*, 383, **1996**, 145.
- [4] J. M. Hernandez, F. Torres, J. Tejada, E. Molins, *Phys. Rev. B.*, 16, **2002**, 1407.
- [5] D. Ruiz-Molina, G. Christou, D. N. Hendrickson, *Mol. Cryst. Liq. Cryst.* 343, **2000**, 335.
- [6] M. Soler, W. Wernsdorfer, Z. M. Sun, J. C. Huffman, D. N. Hendrickson, G. Christou, *Chem. Commun.* **2003**, 2672.
- [7] (a) J. Jung, M. Perrut, *Ind. Eng. Chem. Res.*, 25, **2003**, 6375. (b) D.W. Matson, J.L. Fulton, R.C. Petersen, R.D. Smith, *Ind. Eng. Chem. Res.* 26, **1987**, 2298. (c) R.Thiering, F. Dehgani, N.R. Foster, *J. Supercrit. Fluids*, 21, **2001**, 159. (d) N. Ventosa, S. Sala, J. Veciana, J. Llibre, J. Torres, *Cryst. Growth & Design*, 1, **2001**, 299.
- [8] M. Munto, J. Gomez, J. Campo, N. Ventosa, J. Veciana, D. Ruiz-Molina, *Chem. Commun.* **2005** (submitted)